HTML ABSTRACT + LINKS

Computer-aided simulation of a rotary sputtering magnetron

Qi Hua Fan[a] and J. J. Gracio
Department of Mechanical Engineering, Center for Mechanical Technology and Automation, University of Aveiro, 3810 Aveiro, Portugal

Li Qin Zhou
Department of Materials Science and Engineering, The University of Michigan, Ann Arbor, Michigan 48109

(Received 3 November 2003; accepted 4 March 2004)

In the past, computer-aided simulation of sputtering magnetron has been applied mainly to planar cathodes with flat target surfaces. In this work, we have simulated the target erosion profile of a cylindrical rotary magnetron by tracing electron trajectories and predicting ionization distribution. The electric potential is prescribed as a radial function. A fourth-order Runge–Kutta method is used to solve the electron movement equations, and a Monte Carlo method is employed to predict electron/Ar collision. It is shown that the simulation can predict the target erosion with reasonable accuracy. © *2004 American Institute of Physics.* [DOI: 10.1063/1.1715133]

I. INTRODUCTION

Since being developed in the late 1970s, magnetron sputtering has been widely used for thin-film deposition (see, e.g., Refs. 1–9). A magnetron cathode is the core of the sputtering system. The most popular cathode is a planar magnetron characterized by relatively simple configuration with flat target surface. A major problem with planar magnetron sputtering is the low utilization of target. In the past years, much effort has been devoted to this issue, and the target utilization has been significantly improved.[10–20] One promising solution is to use a rotary magnetron,[21] in which a cylindrical target rotates slowly, while the magnet assembly is set statically inside the target cylinder, as shown in Fig. 1. Such a rotary magnetron usually yields utilization higher than 70%, which is usually not achieved by a planar magnetron. In addition, the rotary cathode enables a full etching of the target surface. This makes the sputtering process very stable, especially during reactive deposition.

To optimize the performance of the rotary cathode, the magnetic field needs to be carefully designed to meet the requirements for various coatings. For example, an unbalanced magnetic field may be needed to modify the film structure. Since the target is not flat, it is difficult to empirically predict the target erosion by only comparing the magnetic flux density over the target surface. Therefore, computer-aided simulation of the target erosion is quite necessary in terms of efficiency and economy.

Previous efforts in magnetron simulation have been concentrated mainly on the planar cathode with a flat target surface.[22–27] The simulation is able to accurately predict electron trajectory, ionization distribution, space-charge distribution, electric potential, target erosion, etc. It has become an important means of magnetron design. In this work, we apply the principle of planar magnetron simulation to a rotary cathode that has a cylindrical target. The purpose is to verify the validity of the simulation methodology for a nonflat target. Experiments are conducted to compare the erosion profile in a cylindrical target with the simulation results.

II. EXPERIMENTS

In this work, we investigate the straight section of a rotary magnetron, as shown in Fig. 1. The straight section includes a cylindrical target, a set of NdFeB permanent magnets, and a magnetically permeable steel yoke. The dimensions of these parts are also shown in the figure together with the magnetization direction of each magnet. Sputtering was conducted in Ar at a typical gas pressure of 4 mTorr. The cylindrical Cu target was ~1800 mm in length with an outer diameter of 142.24 mm. The target thickness was 6 mm and the sputtering process stopped of about half of the target lifetime. It should be noted that in this experiment the target was set static without rotating, as we are interested in comparing the erosion pattern in the cylindrical target with simulation result. In practical process the cathode rotates at a speed of two turns per minute to realize uniform erosion of the target surface. The erosion depth in the middle region of the target was measured using a profiler and used to compare with simulation results.

III. SIMULATION METHOD

The movement of a charged particle in the magnetic and electric fields is governed by the ordinary differential equation

$$\frac{d(m\mathbf{v})}{dt}=q(\mathbf{E}+\mathbf{v}\times\mathbf{B}), \quad (1)$$

where m is the mass, $\mathbf{v}$ the velocity vector, t time, q the charge, $\mathbf{E}$ the electric field vector, $\mathbf{B}$ the magnetic field vector.[28] To trace electron trajectories, a fourth-order Runge–Kutta method is used to solve Eq. (1) in combination with the fact that the velocity vector is the derivative of a position vector.[29] The numerical simulation takes the magnetic and electric fields as input. As we are investigating the straight

[a]Author to whom correspondence should be addressed; electronic mail: fan@mec.ua.pt

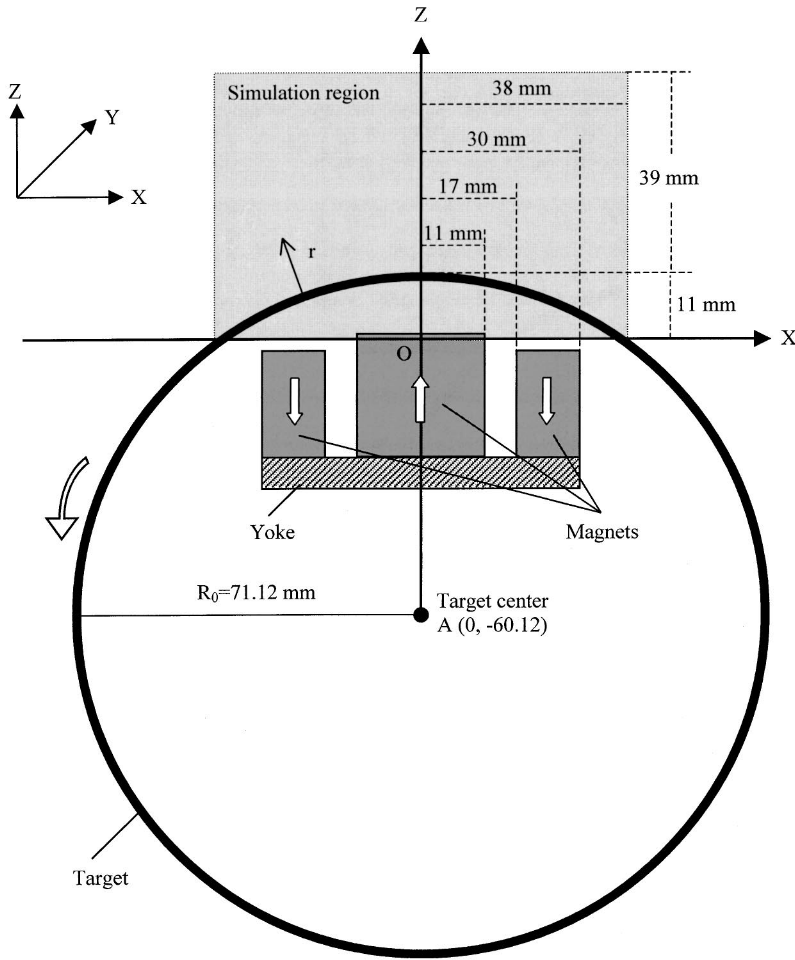

FIG. 1. Straight section of a rotary magnetron cathode used for simulation and test.

section of the rotary cathode, the magnetic field over the target surface can be treated as a two-dimensional (2D) problem and is, therefore, calculated using a 2D magnetic field simulation software, Finite Element Method Magnetics.[30] The field along the y axis (refer coordinates in Fig. 1) is assumed to be identical in the straight portion of the cathode that is far away from the end region. The magnetic field data is tabulated with a 0.5 mm grid in space. The field value between the grids is interpolated. The magnetic field has little effect on the trajectory of an Ar^+ ion as Ar^+ is too heavy. Thus, the Ar^+ ions just follow the electric field and strike the target surface, causing sputtering of the target materials.

The electric potential Φ is prescribed in a format similar to a planar magnetron.[27] The difference is that, for the cylindrical rotary magnetron, the potential is a function of the radial distance r from the target surface. The potential Φ, consisting of a sheath and a presheath, satisfies Poisson's equation

$$\frac{d^2\Phi}{dr^2}=-\frac{e}{\epsilon_0}(n_i-n_e), \tag{2}$$

where e is the charge of electron, ϵ_0 is the permittivity of vacuum, and n_i and n_e are the densities of Ar^+ ions and electrons, respectively. Plasma prevails in the presheath region; that is, $n_i=n_e$. Thus, Φ is a linear function of r in presheath

$$\Phi(r)=-\alpha\Phi_0\frac{(R-r)}{(R-r_s)}, \tag{3}$$

where α is a constant, Φ_0 is the voltage applied to the cathode, being 385 V under normal operation conditions for the rotary cathode, R is target–substrate distance (50 mm in the present simulation), and r_s is the thickness of the sheath. From Bohm's criterion, we have $\alpha\Phi_0=kT_e/2e$, where k is Boltzmann's constant, and T_e is the electron temperature with a typical value of 2.5 eV.[31,32] The thickness of the sheath is estimated from Child–Langmuir law, to be about $r_s=2.5$ mm. Since r_s is a very short distance, $\Phi(r)$ can be approximately expressed by a third-order polynomial in the sheath, as

$$\Phi=-\Phi_0(1+c_1r+c_2r^2+c_3r^3), \tag{4}$$

where c_1, c_2 and c_3 are constants that can be determined from Eqs. (3) and (4) so that Φ, Φ', and Φ'' are connected smoothly at $r=r_s$, respectively. The electric field $\mathbf{E}$ can be derived from the potential $\Phi(r)$, as

$$\mathbf{E}(r)=-\frac{d\Phi(r)}{dr}. \tag{5}$$

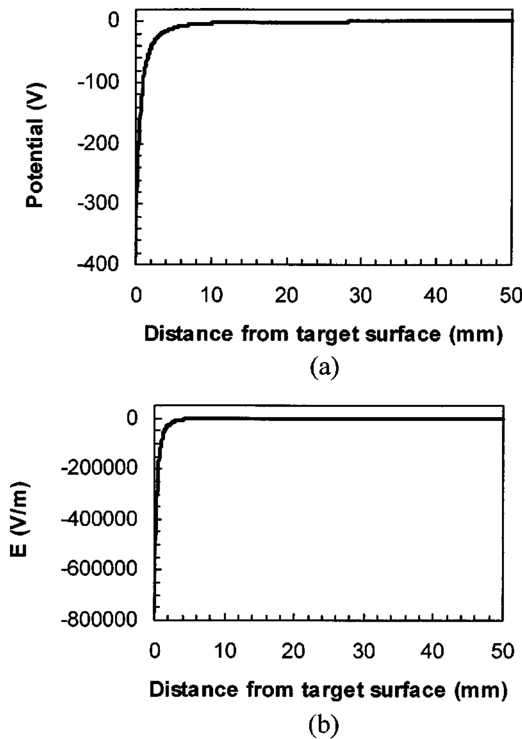

FIG. 2. (a) Electric potential U and (b) electric field $\mathbf{E}$ used in the simulation.

Figure 2 shows the derived electric field and potential used in this simulation.

To predict the target erosion, a Monte Carlo method is used to determine the electron/Ar collision according to the total cross section.[33–35] High-energy electrons are either emitted from the target surface, known as secondary electrons, or are born mainly in the sheath region as a consequence of ionization. In the Monte Carlo simulation, the electrons are started at random positions. Three types of collisions are considered: elastic scattering, excitation, and ionization. All these collisions result in the change of the electron's energy and/or its direction of velocity. The energy losses for ionization and excitation are 15.8 and 11.6 eV, respectively, while energy loss from elastic scattering is ignored. The direction of a post-collision velocity of the electron is determined by the differential scattering cross section, which varies with energy.[36] The ionization positions are recorded and used to predict target erosion. In our simulation, ionization through two-step and multistep processes, as well as Coulomb collisions between electrons or between electron and ion, are not considered. This simplification may result in certain error in predicting the discharge characteristics, while its effect on simulated target erosion may be not significant.

The simulation region is: X $(-38,38)$, Y (0,20), and Z (0,50). Once an electron moves out of the area in $X-Z$ plane

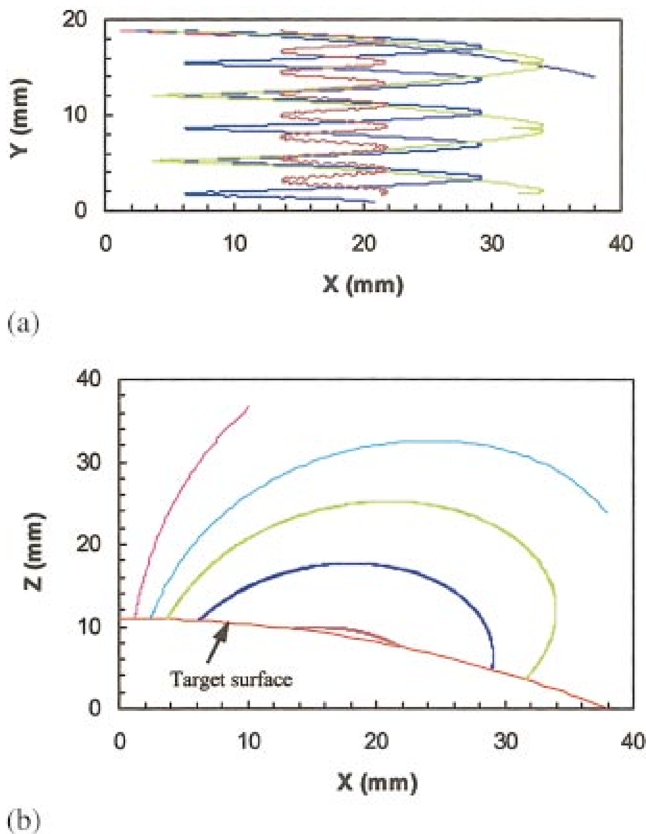

FIG. 3. ⟨Color⟩ Simulated electron trajectories above the rotary cathode surface. (a) top view and (b) side view. The lines in different colors represent the trajectories of electrons starting at different positions in the target surface.

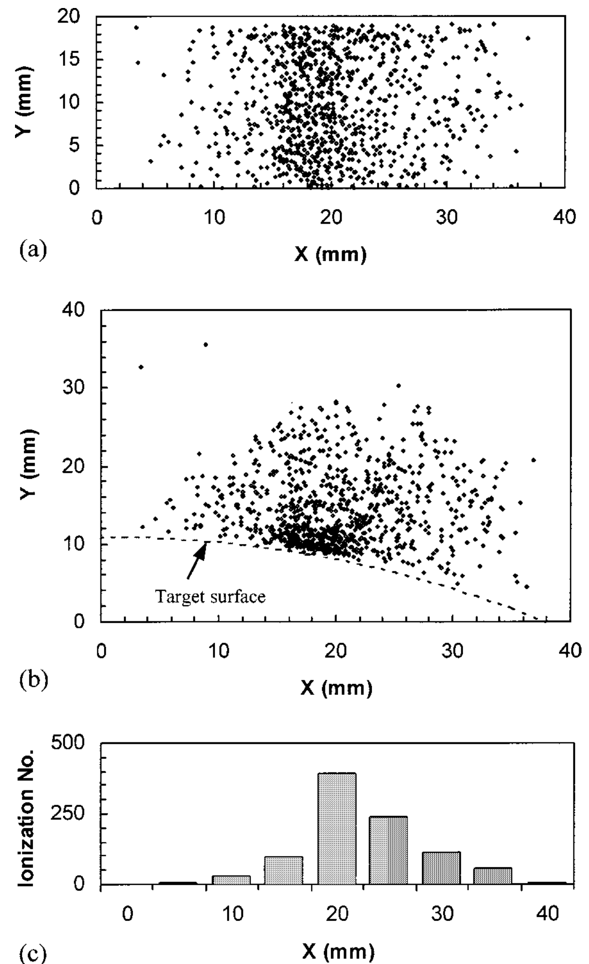

FIG. 4. Simulated ionization distribution in the straightway of the rotary cathode. (a) top view, (b) side view, and (c) ionization number above the target surface.

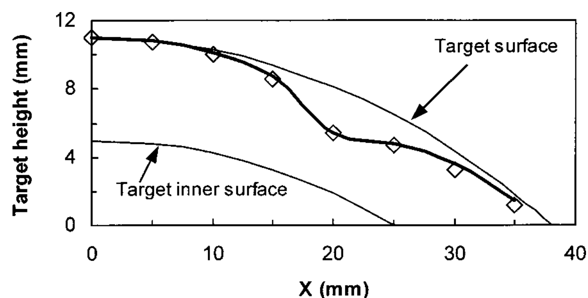

FIG. 5. Simulated (——) and experimental (◇) erosion profiles in the cylindrical target of the rotary magnetron cathode. Note that in this test the target was set still in order to obtain the etching profile. In actual operation, the target rotates and the erosion is uniform.

(refer to Fig. 1), its trajectory is terminated and the next electron is started at a random position. An electron moving out of the *Y* direction is restarted from another end in the *Y* direction with the same *X* and *Z* positions and velocity.

IV. RESULTS AND DISCUSSION

Figure 3 shows simulated electron trajectories above the surface of the cylindrical target. The lines in different colors represent the trajectories of electrons starting at different positions in the target surface. Note that these trajectories are not the same as in the ionization simulation, in which the electron/Ar collisions are taken into account. It can be seen that electrons move in a complicated manner in the three-dimensional space above the target. Once an electron moves out of the simulation region in $X-Z$ plane shown in Fig. 1, it is assumed that this electron escapes from the confinement of the magnetic field.

To predict the target erosion, ionization distribution is simulated. A large number of electrons starting at random positions are traced to ensure statistical accuracy. Ionization positions are predicted using the Monte Carlo method described earlier. Figure 4 shows the simulated ionization distribution. The ionization number along the *X* axis is also shown in Fig. 4. Considering the sputtering yield, the target erosion is simulated according to the Ar^+ ion energy and the ionization locations. The simulated erosion in the cylindrical target is normalized with experimental profile and is shown in Fig. 5. It can be seen that the simulated etching profile is in good agreement with experiment. The results indicate that this simulation method yields reasonable accuracy in predicting target erosion of a cylindrical magnetron.

It should be noted that the cylindrical target rotates in practical process. A more interesting subject is to simulate the erosion uniformity along the *Y* axis (refer to Fig. 1 for coordinates). It is obvious that to predict the erosion uniformity along the *Y* axis, one only needs to compare the sum of the static etching depth along the *X* axis at different *Y* axis positions. This is an essential consideration for modeling a full-sized rotary magnetron, in which the end region is usually eroded at different rate as compared with the straightway. The authors are utilizing the simulation method to optimize a full-sized rotary magnetron with special attention to the magnetic field in the end region.

V. CONCLUSIONS

The erosion profile in the cylindrical target of a rotary cathode can be predicted with reasonable accuracy using a Monte Carlo method by numerically tracing electron trajectories. The simulation utilizes a prescribed electric potential, which is a function of the distance from the target surface and consists of a sheath and a presheath. This method may be readily applied to the design optimization of a full-sized rotary cathode.

ACKNOWLEDGMENT

The authors would like to thank Ed Taylor for his valuable support and suggestions. Also acknowledged is the Foundation for Science and Technology (Portugal) Project POCTI/CTM/35454/2000.

[1] D. B. Fraser, J. Vac. Sci. Technol. **15**, 178 (1978).
[2] J. A. Thornton and A. S. Penfold, in *Thin Film Processes*, edited by J. L. Vassen and W. Kern (Academic, New York, 1978).
[3] J. S. Chapin, United States Patent No. 4,166,018 (28 August, 1979).
[4] J. J. Cuomo and S. M. Rossnagel, J. Vac. Sci. Technol. A **4**, 393 (1986).
[5] S. M. Rossnagel and H. R. Kaufman, J. Vac. Sci. Technol. A **6**, 223 (1988).
[6] R. P. Howson and H. A. Ja'fer, J. Vac. Sci. Technol. A **10**, 1784 (1992).
[7] K. Wasa and S. Hayakawa, *Handbook of Sputter Deposition Technology* (Noyes, New York, 1992).
[8] G. M. Turner, S. M. Rossnagel, and J. J. Cuomo, J. Appl. Phys. **75**, 3611 (1994).
[9] R. A. Powell and S. M. Rossnagel, *PVD for Microelectronics: Sputter Deposition Applied to Semiconductor Manufacturing* (Academic, San Diego, 1999).
[10] K. Abe, S. Kobayyashi, T. Kamel, T. Shimizu, H. Tateishi, and S. Aiuchi, Thin Solid Films **96**, 225 (1982).
[11] C. B. Garrett, United States Patent No. 4,444,643 (24 April 1984).
[12] C. F. Morrison, Jr., United States Patent No. 4,461,688 (24 July 1984).
[13] R. Kukla, T. Krug, R. Ludwig, and K. Wilmes, Vacuum **41**, 1968 (1990).
[14] R. P. Welty, United States Patent No. 4,892,633 (9 January 1990).
[15] Q. H. Fan, Y. Hong, H. Chen, and X. Chen, Thin Solid Films **229**, 51 (1993).
[16] B. W. Manley, United States Patent No. 5,262,028 (16 November 1993).
[17] N. Hosokawa and T. Kobayashi, United States Patent No. 5,458,759 (17 October 1995).
[18] D. G. Teer, J. Hampshire, V. Fox, and V. Bellido-Gonzalez, Surf. Coat. Technol. **94–95**, 572 (1997).
[19] J. Musil, J. Vac. Sci. Technol. A **17**, 555 (1999).
[20] D. Haas, W. Buschbeck, and J. Krempel-Hesse, United States Patent No. 6,207,028 (27 March 2001).
[21] M. Wright and T. Beardow, J. Vac. Sci. Technol. A **4**, 388 (1986).
[22] T. E. Sheridan, M. J. Goeckner, and J. Goree, J. Vac. Sci. Technol. A **8**, 30 (1990).
[23] S. Ido and K. Nakamura, Jpn. J. Appl. Phys. **32**, 5698 (1993).
[24] K. Nanbu and I. Warabioka, Prog. Astronaut. Aeronaut. **160**, 428 (1994).
[25] S. Kondo and K. Nanbu, J. Phys. D **32**, 1142 (1999).
[26] E. Shidoji, H. Ohtake, N. Nakano, and T. Makabe, Jpn. J. Appl. Phys., Part 1 **38**, 2131 (1999).
[27] Qi Hua Fan, L. Q. Zhou, and J. Gracio, J. Phys. D **36**, 244 (2003).
[28] J. L. Shohet, *The Plasma State* (Academic, New York, 1971), p. 39.
[29] S. S. M. Wong, *Computational Methods in Physics and Engineering* (World Scientific, Singapore, 1997), p. 384.
[30] Software package may be found at http://femm.berlios.de/
[31] R. F. Bunshah, *Deposition Technologies for Films and Coatings* (Noyes, New Jersey, 1982), p. 32.
[32] F. Guimarães, J. Almeida, and J. Bretagne, J. Vac. Sci. Technol. A **9**, 133 (1991).
[33] M. E. J. Newman and G. T. Barkema, *Monte Carlo Methods in Statistical Physics* (Clarendon, Oxford, 1999).
[34] J. Bretagne, G. Callede, M. Legentil, and V. Puech, J. Phys. D **19**, 761 (1986).
[35] V. Puech and L. Torchin, J. Phys. D **19**, 2309 (1986).
[36] S. N. Nahar and J. M. Wadehra, Phys. Rev. A **35**, 2051 (1987).